

KAPL-P-000047
(K96048)

CONF-9605348--

RECENT PROGRESS IN INGAASSB/GASB TPV DEVICES

Z.A. Shellenbarger, M.G. Mauk, L.C. DiNetta, G.W. Charache

May 1996

NOTICE

This report was prepared as an account of work sponsored by the United States Government. Neither the United States, nor the United States Department of Energy, nor any of their employees, nor any of their contractors, subcontractors, or their employees, makes any warranty, express or implied, or assumes any legal liability or responsibility for the accuracy, completeness or usefulness of any information, apparatus, product or process disclosed, or represents that its use would not infringe privately owned rights.

KAPL ATOMIC POWER LABORATORY

SCHENECTADY, NEW YORK 12301

Operated for the U. S. Department of Energy
by KAPL, Inc. a Lockheed Martin company

[Signature] **MASTER**

DISTRIBUTION OF THIS DOCUMENT IS UNLIMITED

DISCLAIMER

This report was prepared as an account of work sponsored by an agency of the United States Government. Neither the United States Government nor any agency thereof, nor any of their employees, makes any warranty, express or implied, or assumes any legal liability or responsibility for the accuracy, completeness, or usefulness of any information, apparatus, product, or process disclosed, or represents that its use would not infringe privately owned rights. Reference herein to any specific commercial product, process, or service by trade name, trademark, manufacturer, or otherwise does not necessarily constitute or imply its endorsement, recommendation, or favoring by the United States Government or any agency thereof. The views and opinions of authors expressed herein do not necessarily state or reflect those of the United States Government or any agency thereof.

DISCLAIMER

**Portions of this document may be illegible
in electronic image products. Images are
produced from the best available original
document.**

Recent Progress in InGaAsSb/GaSb TPV Devices

Z.A. SHELLENBARGER, M.G. MAUK, and L.C. DiNETTA

AstroPower, Inc. Solar Park, Newark, DE 19716-2000

G.W. CHARACHE

Lockheed Martin Corp. P.O. Box 1072, Schenectady, NY 12301-1072

SUMMARY

AstroPower is developing InGaAsSb thermophotovoltaic (TPV) devices. This photovoltaic cell is a two-layer epitaxial InGaAsSb structure formed by liquid-phase epitaxy on a GaSb substrate. The (direct) bandgap of the $In_{1-x}Ga_xAs_{1-y}Sb_y$ alloy is 0.50 to 0.55 eV, depending on its exact alloy composition (x, y); and is closely lattice-matched to the GaSb substrate. The use of the quaternary alloy, as opposed to a ternary alloy — such as, for example, InGaAs/InP — permits low bandgap devices optimized for 1000 to 1500 °C thermal sources with, at the same time, near-exact lattice matching to the GaSb substrate. Lattice matching is important since even a small degree of lattice mismatch degrades device performance and reliability and increases processing complexity.

Internal quantum efficiencies as high as 95% have been measured at a wavelength of 2 microns. At 1 micron wavelengths, internal quantum efficiencies of 55% have been observed. The open-circuit voltage at currents of 0.3 A/cm² is 0.220 volts and 0.260 V for current densities of 2 A/cm². Fill factors of 56% have been measured at 80 mA/cm². However, as current density increases there is some decrease in fill factor. Our results to date show that the GaSb-based quaternary compounds provide a viable and high performance energy conversion solution for thermophotovoltaic systems operating with 1000 to 1500 °C source temperatures.

1. INTRODUCTION

We report our latest results on InGaAsSb thermophotovoltaic (TPV) cells. TPVs are *p-n* junction semiconductor devices that convert photons emitted by a heated source directly into electrical power. For TPV systems utilizing thermal radiation from an emitter heated at 1000 to 1500 °C, there is a need for low-bandgap cells with a high spectral response in the range of 1500 to 2500 nm wavelength. This implies a TPV cell with a bandgap of ~0.5 eV. One important potential application is the radioisotope General Purpose Heat Source (GPHS) where 1100 °C blackbody radiation can be used for thermophotovoltaic energy conversion. In this paper we describe high-efficiency TPV devices based on lattice matched $In_{0.04}Ga_{0.92}As_{0.07}Sb_{0.93}$ ($E_g = 0.53$ eV) epitaxial layers on GaSb substrates. To our knowledge, this is the first report of the InGaAsSb quaternary alloy applied to TPV devices.

Several theoretical studies have indicated that photovoltaic cells based on the InGaAsSb quaternary alloy are good candidates for TPV applications that require high spectral response in the 1500 to 2500 nm wavelength range. Depending on its alloy composition (x, y), the direct bandgap of the $In_{1-x}Ga_xAs_{1-y}Sb_y$ alloy varies from 0.18 eV (InSb) to 1.43 eV (GaAs). The quaternary alloy can be closely lattice-matched to the GaSb substrate provided the composition is restrained to values such that $y \approx 0.1 + 0.9 x$. With this lattice matching condition, the

bandgap of the quaternary alloy ranges from approximately 0.3 to 0.7 eV. However, there is a further limitation due to a wide solid-phase miscibility gap in this quaternary at typical growth temperatures. The miscibility gap evidently precludes bandgaps in the range of 0.35 to 0.5 eV. Therefore, for the spectral range of interest, we assume the lowest attainable bandgap is 0.50 to 0.52 eV. This bandgap range corresponds to an optical absorption edge of 2380 to 2480 nanometers.

It is worth emphasizing that the use of the quaternary alloy, as opposed to a ternary alloy—such as, for example, InGaAs—provides the needed bandgap with, at the same time, near-exact lattice matching to the GaSb substrate. Lattice-matching is important since even a small degree of lattice mismatch degrades device performance and reliability. Although there are epitaxy techniques to partially ameliorate effects associated with lattice mismatch of ternary alloy layers on binary substrates (e.g. defect-filtering superlattices, interrupted growth regimens, etc.). We believe the use of the quaternary alloy to avoid lattice mismatch altogether is a simpler and more effective approach.

The TPV device we are making is a two-layer epitaxial InGaAsSb structure formed by liquid-phase epitaxy on a GaSb substrate at a growth temperature of 515 °C. Liquid-Phase Epitaxy (LPE) is a well-established technology for III-V compound semiconductor devices. A major advantage of LPE for this application is the high material quality, and more specifically, the long minority carrier diffusion lengths, that can be achieved. This results in devices which are equal or superior in performance to those made by other epitaxy processes such as molecular beam epitaxy (MBE) or metal organic chemical vapor deposition (MOCVD). Another major advantage is that LPE is a simple, inexpensive, and safe method for semiconductor device fabrication. Significantly, the LPE process does not require or produce any highly toxic or dangerous substances—in contrast to MOCVD. Also, the epitaxial growth rate with InGaAsSb LPE is ~2 microns/minute which is ten to hundred times faster than MOCVD or MBE. We have successfully scaled up the LPE process for epitaxial growth in a semi-continuous mode on 3-inch diameter wafers. This, combined with the high growth rates, will dramatically improve the manufacturing throughput compared to traditional and more costly epitaxy processes. Our objective is to develop an epitaxial growth technology to produce low-cost, large-area, high efficiency TPV devices.

2. EPITAXIAL GROWTH AND FABRICATION OF InGaAsSb TPV CELLS

InGaAsSb photodiodes, light-emitting diodes, and double heterostructure injection lasers made by liquid-phase epitaxy have been previously reported. We have adapted this technology for the production of InGaAsSb TPV cells.

We use a standard horizontal slideboat technique for the liquid-phase epitaxial growth of the InGaAsSb. The graphite slideboat is situated in a sealed quartz tube placed in a microprocessor-controlled, programmable, three-zone tube furnace. The growth ambient is palladium-diffused hydrogen at atmospheric pressure with a flow rate of 300 ml/min.

The substrates are 500-micron thick, chemically polished (100) oriented, *n*-type GaSb wafers obtained from MCP Wafer Technology, Ltd. (Milton Keynes, UK) or Firebird Semiconductor, Ltd. (Trail, BC, Canada). Substrates are doped to $3.5 \times 10^{17} \text{ cm}^{-3}$ with tellurium. The substrate resistivity is $9 \times 10^3 \Omega \cdot \text{cm}$, and the average etch-pit density is approximately 1000 cm^{-2} .

The growth solutions are indium ($x_{\text{In}}=0.59$), gallium ($x_{\text{Ga}}=0.19$), antimony ($x_{\text{Sb}}=0.21$), and arsenic ($x_{\text{As}}=0.01$). The melts are formulated with 3- to 5-mm shot of high purity (99.9999%) indium, gallium, and antimony metals and arsenic added as undoped InAs polycrystalline material. The total weight of the melt is about 10 g. Prior to growth, the melts are baked out at 700 °C for fifteen hours under flowing hydrogen to de-oxidize the metallic melt components and outgas residual impurities. After bake-out, appropriate dopant impurities are added to each melt. The first melt for the growth of the *n*-type InGaAsSb base layer contains tin or tellurium. The small amount of Te needed to dope the layer (atomic fraction in the melt $\geq 10^{-5}$) is problematic. For reproducible doping, a weighable amount of Te is added as 100 to 200 mg of Te-doped GaSb ($C_{\text{Te}}=10^{19} \text{ cm}^{-3}$). Tin is added to

the melt as 10 to 200 mg of high purity shot. Our preliminary results (Section 3) suggest that high *n*-type doping concentrations can be achieved more readily with tin than with tellurium. However, the relatively high liquid-phase concentration of tin alters the melt composition needed to grow the lattice-matched InGaAsSb quaternary with the desired bandgap. For higher tin doping levels, we will need to re-optimize the melt compositions to include the effects of dilution with additional tin. This will require a phase equilibria analysis and model of a 5-component system (In-Ga-As-Sb-Sn). The second melt for the growth of the *p*-type emitter contains 5 to 100 mg germanium. Presently, we are beginning a more detailed and systematic characterization of impurity segregation and doping in the In-Ga-As-Sb quaternary system with the aim of achieving better control and a greater range of doping concentrations.

The melts are equilibrated for 1 hour at 530 °C and then cooled at a rate of 0.7 °C/min. At 515 °C, the substrate is contacted with the first melt for two minutes to grow a 5-micron thick *n*-type InGaAsSb base layer. Next, the substrate is moved to the second melt for 5 seconds to grow a 0.3-micron thick *p*-type InGaAsSb emitter layer.

Front and back ohmic contacts are formed on the epitaxial InGaAsSb/GaSb structure by standard processing techniques. The back of the substrate is metallized by plating with a 200-nm thick electron-beam evaporated Au:Ge:Au:Ni layer and alloyed at 300 °C. The front contact is a grid of 10-micron wide metallization lines with 100-micron spacing and a single 1-mm wide center busbar. The grid is formed by a photolithography lift-off process with a 200-nm thick electron-beam evaporated Au:Zn:Au metallization. The front grid is thickened to 5 microns by gold electroplating. The front contact is not sintered. The substrate is masked and patterned to define a 1 cm x 1 cm device and isolation etched with a potassium iodide - iodine "gold" etch. Most of our TPV cells are 1 cm x 1 cm in area; although larger cells (2 cm x 2 cm) with comparable performance have also been made. In order to simplify the spectral response analysis, we elected not to apply any anti-reflection coatings to the cells. FIGURE 1 is a top-view photograph of a 1 cm x 1 cm InGaAsSb TPV cell.

3. TPV DESIGN AND OPTIMIZATION

FIGURE 2 shows the TPV device design in cross-section. The fabricated cells have a 0.3 to 0.5 micron thick *p*-type emitter with a Ge concentration of approximately 10^{19} cm⁻³, as indicated by Secondary Ion Mass Spectroscopy (SIMS). A thicker, more heavily doped *p*-layer will reduce the sheet resistance of the emitter and therefore improve the fill-factor, but will tend to reduce spectral response due to higher free-carrier absorption and increased sensitivity to front surface minority carrier recombination.

The base thickness in our cells ranges from 3 to 5 microns with a Te or Sn concentration of about 10^{15} to 10^{18} cm⁻³, as determined from capacitance-voltage measurements and SIMS. FIGURE 3 shows the SIMS depth profile indicating the abruptness of the *p*-*n* junction and the depth uniformity of the doping concentrations. There is apparently very little smearing of the doping profile due to diffusion or segregation of dopants. Discrepancies between the Te dopant concentration measured by SIMS (total impurity concentration) and that implied by capacitance-voltage measurements (net donor concentration) indicate that much of the Te is either not ionized or else is compensated. This is a common problem in Te doping of III-V semiconductors, especially in GaSb-based materials, and is probably due to the formation of electrically inactive telluride complexes or compounds in the material. Increasing the Te concentration in the melt showed a "saturation effect" in that the Te doping level did not increase in proportion to the Te concentration in the liquid phase. Our most recent devices incorporate tin as the *n*-type base dopant and have base dopings targeted around 10^{17} cm⁻³. Modeling indicates that base dopings in this range will yield the optimum open-circuit voltages and short-wavelength quantum efficiencies.

4. TPV DEVICE EVALUATION

We present external and internal spectral response and current-voltage characteristics for 1 cm x 1 cm $p\text{-In}_{0.08}\text{Ga}_{0.92}\text{As}_{0.07}\text{Sb}_{0.93}\text{-Ge}$ / $n\text{-In}_{0.08}\text{Ga}_{0.92}\text{As}_{0.07}\text{Sb}_{0.93}\text{-Te}$ (or Sn) epitaxial cells on an $n\text{-GaSb:Te}$ substrate produced as described above. The *external* spectral response of a typical InGaAsSb TPV cell is shown in FIGURE 4. FIGURE 5 shows the corresponding *internal* spectral response. The lower external spectral response is due to grid shading and reflection of incident light from the uncoated InGaAsSb emitter surface. The grid shading is 18.2%. The absorption edge implied by the spectral response measurements of a number of samples ranged from approximately 2200 to 2250 nm. At a wavelength of 2000 nm, internal quantum efficiencies as high as 95% have been measured, and at a wavelength of 1 micron, internal quantum efficiencies of almost 55% have been observed. The internal quantum efficiency averaged over the spectral region from 1 to 2 microns wavelength is 60%. (It should be noted that for the intended TPV applications, the response of the cell for wavelengths less than 1.5 microns is not important.)

The 1 cm x 1 cm InGaAsSb TPV cells were tested under simulated infrared light using a ZnSe-filtered tungsten source (Carley Lamps, Inc., Torrance, CA) with a spectral emission in the 800 to 3000 nm wavelength range. Under an illumination intensity corresponding to a short-circuit current density of 2 A/cm^2 , open-circuit voltages as high as 0.280 volts have been measured. FIGURE 6 shows the current-voltage characteristics of a 1 cm x 1 cm InGaAsSb TPV cell under an infrared illumination intensity that yields a short-circuit current density of 62.4 mA/cm^2 and a open-circuit voltage of 0.178 V. The fill-factor is 0.57. To date, the best fill-factors observed are less than 0.6. We believe that one cause of the somewhat low fill-factors is series resistance, which is discussed further in the next section. FIGURE 7 shows open-circuit voltage vs. short-circuit current for varying light intensity. The open-circuit voltage increases logarithmically with illumination intensity and an open-circuit voltage of $\sim 0.250 \text{ V}$ is reached for current densities of 1 A/cm^2 . The diode ideality factor in the voltage range of 0.1 to 0.25 V is close to 2, implying that high injection is dominant in this voltage range.

5. CONCLUSION AND DISCUSSION

Our results to date have demonstrated the potential of InGaAsSb TPV devices made by liquid-phase epitaxy. We believe there is still room for substantial efficiency enhancements in these devices by optimization of the doping levels and layer thicknesses. Further improvements might include wide bandgap lattice-matched AlGaAsSb window layers for front surface passivation, and AlGaAsSb back-surface field cladding layers to reduce the reverse saturation current and thereby increase the open-circuit voltage. Highly doped contact layers will provide lower series resistance, as will substrate thinning. Lower series resistance will lead to higher fill factors. Thinning the substrate will also improve heat sinking of the device.

The required performance of a TPV device is dependent on its system application. Spectral control of thermal emitters, the use of selective filters and reflectors, heat transfer, and photon recycling effects need to be included in the device design and system optimization. These considerations are not usually relevant for conventional photovoltaic devices and therefore the design and optimization rules for TPVs will be significantly different than those for solar cells. For example, grid obscuration and reflection are not necessarily losses in TPV systems if photons reflected from the front surface are re-absorbed by the emitter. Our next generation of InGaAsSb TPV devices will incorporate design features to fully exploit photon recycling effects.

REFERENCES

A. ANDASPAEVA, A.N. BARANOV, A. GUSEINOV, A.N. IMENKOV, L.M. LITVAK, G.M. FILARETOVA, and Y.P. YAKOVLEV, "Highly Efficient GaInAsSb Light-Emitting Diodes ($\lambda = 2.2 \text{ m}$, $\eta = 4\%$, $T = 300\text{K}$)" Soviet Technical Physics Letters 14, 5 (1988) 377-378.

M. ASTLES, H. HILL, A.J. WILLIAMS, P.J. WRIGHT, and M.L. YOUNG, "Studies of the $\text{Ga}_{1-x}\text{In}_x\text{As}_{1-y}\text{Sb}_y$ Quaternary Alloy System I. Liquid-Phase Epitaxial Growth and Assessment" *J. Electronic Materials* 15, 1 (1986) 41-49.

A.N. BARANOV, A.M. LITVAK, K.D. MOISEEV, N.A. CHARYKOV, and V.V. SHERTSNEV, "Melt-Solid Phase Equilibria in the $\text{In}-\text{Ga}-\text{As}-\text{Sb}$ and $\text{In}-\text{As}-\text{P}-\text{Sb}$ Systems" *Russian J. Physical Chemistry* 64, 6 (1990) 884-886.

A.N. BARANOV, V.V. KUZNETSOV, E.R. RUBTSOV, Y.P. YAKOVLEV, and A.A. GUSEINOV, "Kinetics of Crystallization of the $\text{Ga}_x\text{In}_{1-x}\text{As}_{1-y}\text{Sb}_{1-y}$ Solid Solutions from the Liquid" *Russian J. Physical Chemistry* 65, 12 (1991) 1713-1716.

C. CANEAU, A.K. SRIVASTAVA, A.G. DENTAI, J.L. ZYSKIND, and M.A. POLLACK, "Room-Temperature $\text{GaInAsSb}/\text{AlGaAsSb}$ DH Injection Lasers at $2.2 \mu\text{m}$ " *Electronics Letters* 21, 18 (1985) 815-817.

J.C. DEWINTER, M.A. POLLACK, A.K. SRIVASTAVA, and J.L. ZYSKIND, "Liquid Phase Epitaxial $\text{Ga}_{1-x}\text{In}_x\text{As}_{1-y}\text{Sb}_{1-y}$ Lattice-Matched to (100) GaSb over the 1.17 to $2.33 \mu\text{m}$ Wavelength Range" *J. Electronic Materials* 14, 6 (1985) 729-747.

A.E. DRAKIN, P.G. ELISEEV, B.N. SVERDLOV, A.E. BOCHKAREV, L.M. DOLGINOV, and L.V. DRUZHININA, "InGaSbAs Injection Lasers" *IEEE J. Quantum Electronics* QE-23, 8 (1987) 1089-1094.

A. JOULLIÉ, F. JIA HUA, F. KAROUTA, and H. MANI, "LPE Growth of $\text{GaInAsSb}/\text{GaSb}$ System: The Importance of the Sign of the Lattice Mismatch" *J. Crystal Growth* 75 (1986) 309-318.

H. KANO, S. MIYAZAWA, and K. SUGIYAMA, "Liquid-Phase Epitaxy of $\text{Ga}_{1-x}\text{In}_x\text{As}_{1-y}\text{Sb}_{1-y}$ Quaternary Alloys on GaSb " *Japanese J. Applied Physics* 18, 11 (1979) 2183-2184.

F. KAROUTA, A. MARBEUF, A. JOLLIÉ, and J.H. FAN, "Low Temperature Phase Diagram of the $\text{Ga}_{1-x}\text{In}_x\text{As}_{1-y}\text{Sb}_{1-y}$ System" *J. Crystal Growth* 79 (1986) 445-450.

N. KOBAYASHI, Y. HORIKOSHI, and C. UEMURA, "Liquid-Phase Epitaxial Growth of $\text{InGaAsSb}/\text{GaSb}$ and $\text{InGaAsSb}/\text{AlGaAsSb}$ DH Wafers" *Japanese J. Applied Physics* 18, 11 (1979) 2169-2170.

J.B. MCNEELY, M.G. MAUK, and L.C. DINETTA, "An $\text{InGaAsSb}/\text{GaSb}$ Photovoltaic Cell by Liquid-Phase Epitaxy for Thermophotovoltaic (TPV) Application" *Proc. 1st NREL Conf. on Thermophotovoltaic Generation of Electricity*, 1994 T.J. COUTTS and J.P. BENNER, eds., (New York: American Institute Physics, 1995) 221-225.

K. NAKAJIMA, K. OSAMURA, K. YASUDA, and Y. MURAKAMI, "The Pseudoquaternary Phase Diagram of the $\text{Ga}-\text{In}-\text{As}-\text{Sb}$ System" *J. Crystal Growth* 41 (1977) 87-92.

N. KOBAYASHI and Y. HORIKOSHI, "Pseudoquaternary Phase Diagram Calculation of $\text{In}_{1-x}\text{Ga}_x\text{As}_{1-y}\text{Sb}_y$ Quaternary System" *Japanese J. Applied Physics* 21, 1 (1982) 201-202.

K. NAKAJIMA, K. OSAMURA, K. YASUDA, and Y. MURAKAMI, "The Pseudoquaternary Phase Diagram of the $\text{Ga}-\text{In}-\text{As}-\text{Sb}$ System" *J. Crystal Growth* 41 (1977) 87-92.

E. TOURNIÉ, F. PITARD, A. JOULLIÉ, and R. FOURCADE, "High Temperature Liquid Phase Epitaxy of (100) Oriented GaInAsSb Near the Miscibility Gap Boundary" *J. Crystal Growth* 104 (1990) 683-694.

M.M. WANLASS, J.S. WARD, K.A. EMERY, and T.J. COUTTS, "Ga_{1-x}In_xAs Thermophotovoltaic Converters" *IEEE 1st World Conference on Photovoltaic Energy Conversion* (New York: IEEE Press, 1994) 1685-1691.

S. WOJTCZUK, E. GAGNON, L. GEOFFROY, and T. PAROCOS, "In_xGa_{1-x}As Thermophotovoltaic Cell Performance vs. Bandgap" *Proc. 1st NREL Conf. on Thermophotovoltaic Generation of Electricity*, 1994 T.J. COUTTS and J.P. BENNER, eds., (New York: American Institute Physics, 1995) 177-187.

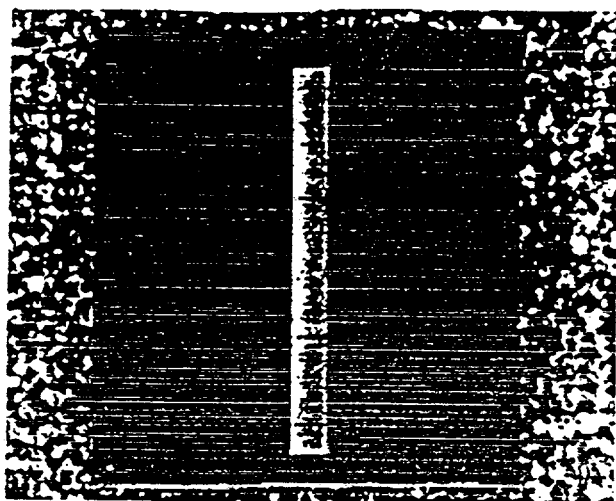


FIGURE 1: Top-view Photograph of a 1 cm x 1 cm InGaAsSb TPV Cell.

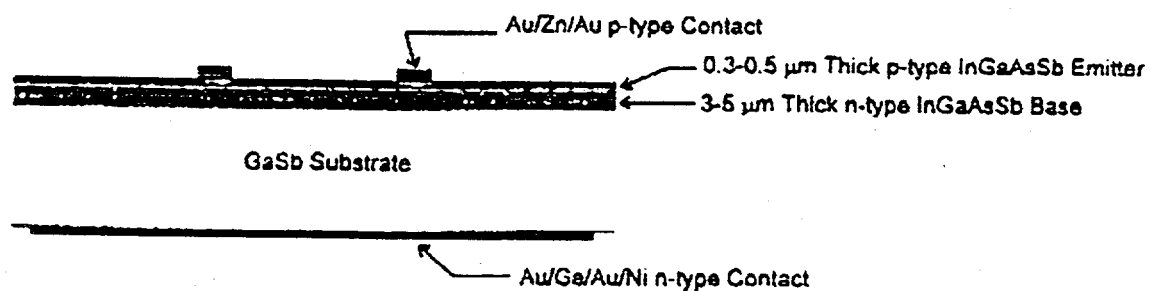


FIGURE 2: InGaAsSb/GaSb p-n Junction Thermophotovoltaic Cell Design.

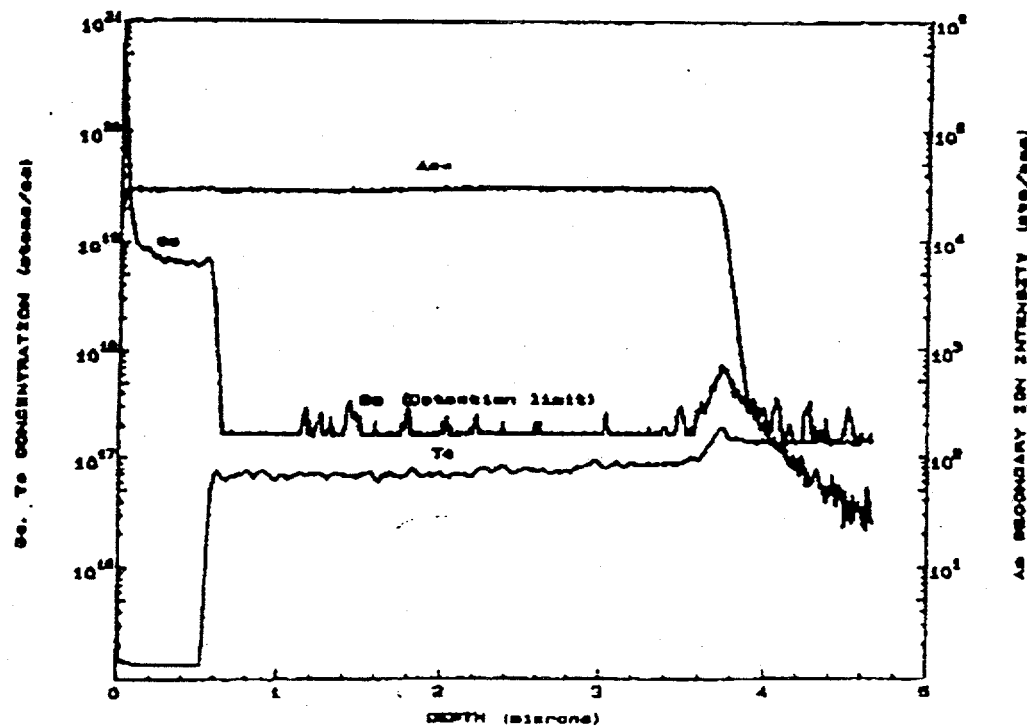


FIGURE 3: SIMS Depth Profile of Doping.

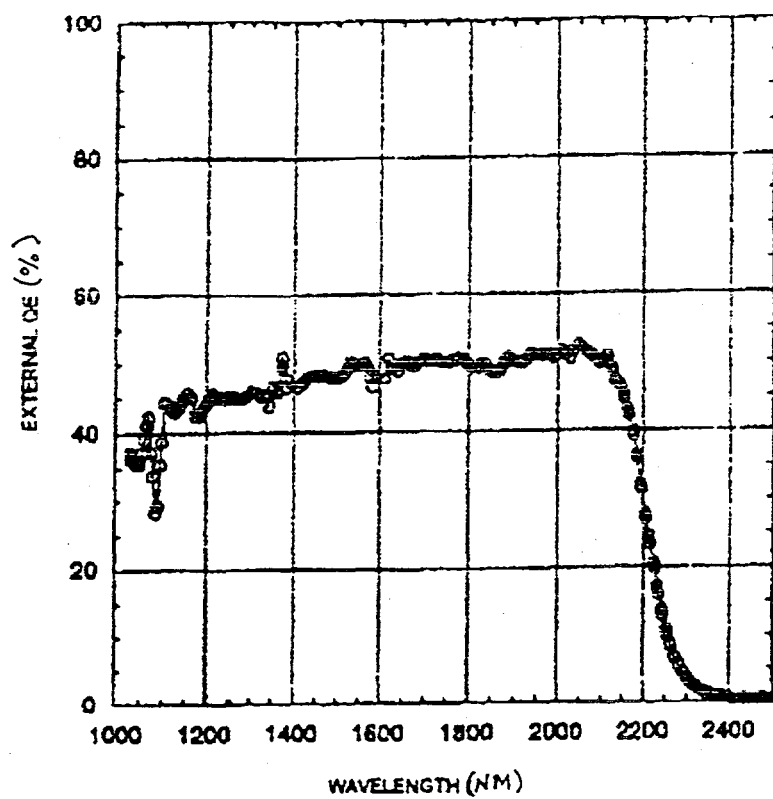


FIGURE 4: External Spectral Response of InGaAsSb/GaSb p-n Junction Thermophotovoltaic Cell.

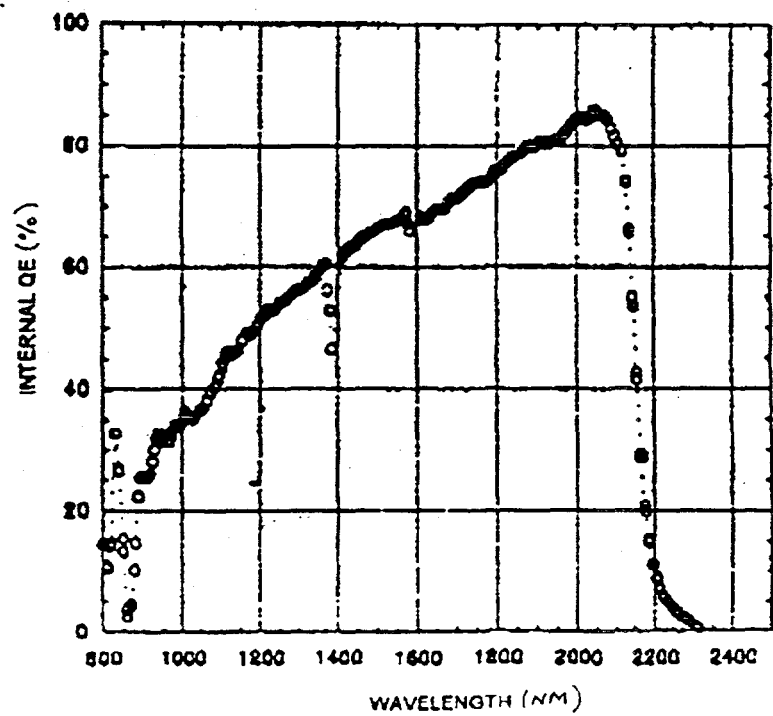


FIGURE 5: Internal Spectral Response of InGaAsSb/GaSb p-n Junction Thermophotovoltaic Cell.

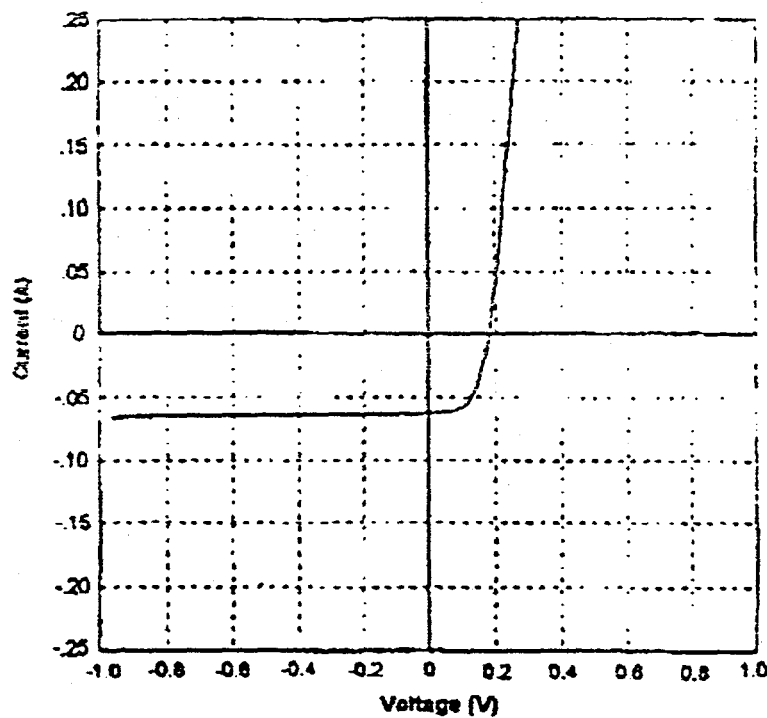


FIGURE 6: Current-Voltage Characteristic of 1 cm x 1 cm InGaAsSb TPV Cell.

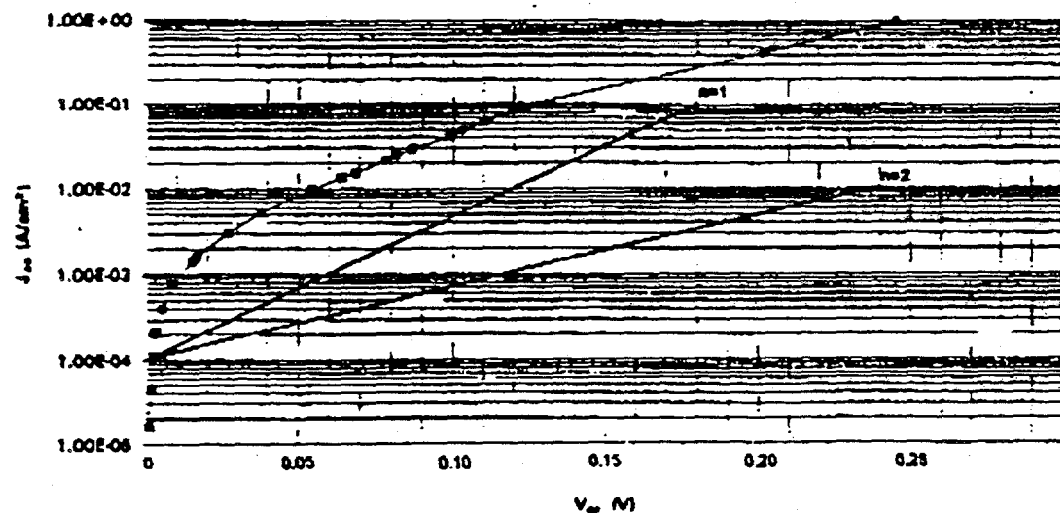


FIGURE 7: Open-Circuit Voltage vs. Short-Circuit Current for InGaAsSb TPV Cell under Varying Illumination Intensity.